Superstable Credit Cycles

Iryna Sushko[a], *Laura Gardini*[b], *Kiminori Matsuyama*[c]

[a]Institute of Mathematics, NASU, Ukraine, [b]University of Urbino, Italy,
[c]Northwestern University, USA

Abstract

We study a particular bifurcation structure observed in the parameter space of a one-dimensional continuous piecewise smooth map generated by the credit cycle model in [23] where the map is defined over the absorbing interval via three functions, one of which is a constant. We show that the flat branch gives rise to superstable cycles whose periodicity regions are ordered according to a modified U-sequence and accumulate to the curves related to homoclinic cycles which represent attractors in Milnor sense. The boundaries of these regions correspond to fold and flip border collision bifurcations as well as persistence border collisions of the related superstable cycles.

1 Introduction

Piecewise smooth dynamical systems have recently become quite a popular topic of research. Such an increasing interest towards nonsmooth dynamics comes both from purely theoretical problems and from various applied fields of science. In fact, particular real processes characterized by "nonsmooth" phenomena (such as sharp switching, impacts, friction, sliding and the like), are quite often modeled by means of piecewise smooth functions, continuous or discontinuous. Among numerous examples the most known are switching electronic circuits, such as DC-DC converters, mechanical systems with impacts or stick-slip motion, relay control systems, etc. (for the related references and further examples from electronics, mechanics, control and other fields see, e.g., the books [9], [5], [39], [13]). Nonsmooth dynamical systems appear naturally also in economics and other social sciences when, for instance, some decision-making process is modeled using logic functions, or if an optimization problem is solved taking into account limited resources or non-negativity constrains, and so forth. For example, several oligopoly models with different kinds of constraints, defined by piecewise smooth maps are considered in the books [33] and [6]. It is worth to mention also the papers dealing with nonsmooth maps related to economic modeling ([11], [18], [23], [32], [14]), financial market modeling ([19], [37], [38]), modeling of multiple-choice ([7], [16], [10]).

The map considered in the present paper arises from an economic application. Namely, we investigate dynamics of the credit cycle model which is a particular case of the more generic model of credit cycles introduced in [23] (see also [24] and [26]). It is described by a one-dimensional (1D for short) continuous piecewise smooth map depending on four parameters and defined by three smooth functions among which one is a constant. This map possesses quite a rich dynamic behavior, and we are interested in understanding how the particular bifurcation structure, observed in its parameter space, is organized. By *bifurcation structure* we mean the partition of the parameter space of a map into regions related to qualitatively similar asymptotic dynamics (see, e.g., [4] where different bifurcation structures characteristic for piecewise smooth 1D maps are discussed). Clearly, the boundaries of such regions are defined by the parameter values corresponding to certain bifurcations. In fact, one of the characteristic features of nonsmooth dynamics is the occurrence of so-called *border collision bifurcation* (BCB for short), first described in [30] (see also [31], [35]). The BCB occurs when, under variation of some parameters, an invariant set (for example, a fixed point or a cycle) collides with a border at which the system changes the function in its definition, and this collision leads to a qualitative change in the dynamics. Such a change can be quite drastic: for example, one can observe the transition from an attracting fixed point to an attracting cycle of any period, or directly to a chaotic attractor, that is impossible in smooth dynamical systems. Thus, the bifurcation structure of the parameter space of a piecewise smooth map may be defined, besides standard "smooth" bifurcations, by the BCBs as well. The possible results of a generic BCB of an attracting cycle of a 1D continuous piecewise smooth map with one border point can be rigorously classified depending on the parameters using *1D BCB normal form,* which is the well known skew tent map defined by two linear functions. The dynamics of the skew tent map are completely described depending on the slopes of the linear branches, that makes it possible to use this map as a normal form (see, e.g., [20], [22], [34]).

Besides nonsmoothness, another notable feature of the considered map is, as already mentioned, the presence in its definition of a flat branch. Obviously, for a piecewise smooth map with a flat branch any cycle with a point on that branch is *superstable* (has 0 eigenvalue), moreover, any initial condition from its basin of attraction is *preperiodic* to such a cycle, that means it is mapped into the cycle in a *finite* number of iterations, namely, as soon as the trajectory reaches the flat branch. From an applied point of view it may be important that superstable cycles related to a flat branch, differently from "smooth" superstable cycles, are persistent under parameter perturbations. That is, in the parameter space there are open regions related to these cycles. Clearly, the boundaries of such periodicity regions can be defined only by BCBs of the related cycles given that the zero eigenvalue doesn't allow any other bifurcation.

The overall bifurcation structure of the parameter space of a piecewise smooth map with a flat branch obviously depends on the particular map (see, e.g., [8], [2], [36]). Our aim is to show that in the parameter space of the considered map the periodicity regions of superstable cycles are organized according

to the well known *U-sequence* (first described in [28], see also [17]) which is characteristic for unimodal maps. It consists of two-letter symbolic sequences ordered for monotonically increasing/decreasing parameter value according to the appearance of the related cycles. We adjust the U-sequence to the considered map by introducing one more letter related to the flat branch, that doesn't influence the basic rule of formation of the U-sequence. However, it is important to emphasize that in the U-sequence of our map the *harmonics* are related to infinite cascades of *flip BCBs* (not of standard flip, or period-doubling, bifurcations), and that the first symbolic sequence in any of such a cascade is related to the cycle born due to *fold BCB* (not to standard fold, or tangent, bifurcation). Considering the overall bifurcation structure in two different parameter planes, we notice that the periodicity regions, ordered in the U-sequence, are accumulating to particular curves. It is natural to suppose that such curves are related to the *homoclinic bifurcations* of the corresponding unstable cycles (cf. with the parameter values of the logistic map related to the homoclinic bifurcations of its unstable cycles, to which periodic windows are accumulating). However, a homoclinic cycle (i.e., the cycle at the moment of its homoclinic bifurcation) of the considered map, being locally unstable, is an attractor in Milnor sense because almost all the initial points of the absorbing interval are mapped into this cycle (see [3] for the discussion of similar attractors in a discontinuous map). That differs from a homoclinic cycle of the logistic map into which only a zero-measure set of initial points (formed by all the preimages of the cycle and called stable set) is mapped.

The plan of the work is as follows. In the next section we define the map, its fixed points and conditions of their stability, specify the region in the parameter space corresponding to the case in which the map is defined over the absorbing interval via all the three functions, introduce the symbolic sequences for the superstable cycles and define their basin of attraction. The main purpose of the present paper is to describe the bifurcation structure in the parameter space of the considered map related to its superstable cycles. In Section 3 we present some numerical results, namely, the 1D and 2D bifurcation diagrams which illustrate the bifurcation structures formed by the periodicity regions related to the superstable cycles. We show that the boundaries of these regions correspond to the fold and flip BCBs, as well as persistence border collisions. Then we present the curves related to the first homoclinic bifurcations of the fixed point and of the 2-cycle, obtained numerically using the conditions of these bifurcations. Examples of homoclinic cycles and their stable sets are also discussed. In Section 4 we recall some basic rules of the formation of the standard U-sequence, and then adjust it to the considered map. In such a way we get the order in which the periodicity regions of the superstable cycles are organized.

2 Description of the map. Preliminaries.

We consider a 4-parameter family of 1D piecewise smooth maps $f : [0,1] \to [0,1]$ defined as follows:

$$f : x \mapsto \ f(x) = \begin{cases} x^{\alpha} & \text{for } 0 \le x \le x_c, \\ \left[\max\left\{\frac{1}{\mu\beta}\left(1-\frac{x}{m}\right), \frac{1}{\beta}\right\}\right]^{\alpha/(1-\alpha)} & \text{for } x > x_c, \end{cases} \tag{1}$$

where α, β, μ and m are real parameters such that

$$0 < \alpha, \mu < 1, \ \beta \equiv B\frac{1-\alpha}{\alpha} > 0, \ 1 < m < \frac{1}{1-\alpha}, \tag{2}$$

and x_c is the *border point* defined by

$$x_c^{1-\alpha} = \frac{1}{\mu\beta}\max\left\{1-\frac{x_c}{m}, \mu\right\}. \tag{3}$$

As we have mentioned in the Introduction, the map f describes a particular case of more generic credit cycle model introduced in [23], namely, the credit cycle model under the assumption of the Cobb-Douglas production function. A preliminary description of the overall bifurcation structure of the map (1) is discussed in [27]. In the present work we focus on the investigation of the bifurcation structure of a particular parameter region related to the superstable cycles of the map f.

Let us first summarize some simple properties of the map and specify the parameter region we are interested in. Depending on the parameters, the map f can be defined by at most three branches which we denote as follows:

$f_L(x) \equiv x^{\alpha}$ (the monotone increasing branch),

$f_M(x) \equiv \left[\frac{1}{\mu\beta}\left(1-\frac{x}{m}\right)\right]^{\alpha/(1-\alpha)}$ (the monotone decreasing branch),

$f_R(x) \equiv \left(\frac{1}{\beta}\right)^{\alpha/(1-\alpha)} \equiv \widehat{x}$ (the flat branch).

The border point x_c can be defined either from $f_L(x_c) = f_M(x_c)$, in which case we denote it as x_l :

$$x_c \equiv x_l : \quad x_l^{1-\alpha} = \left[\frac{1}{\mu\beta}\left(1-\frac{x_l}{m}\right)\right], \tag{4}$$

or from $f_L(x_c) = f_R(x_c)$, in which case we get

$$x_c \equiv x_m = (\widehat{x})^{\frac{1}{\alpha}} = \left(\frac{1}{\beta}\right)^{1/(1-\alpha)}. \tag{5}$$

One more possible border point, denoted x_r, is related to the max function and obtained from $f_M(x_r) = f_R(x_r)$, so that:

$$x_r = m(1-\mu). \tag{6}$$

In the simplest case, defined by the condition $x_m \geq x_r$, that holds for $\beta \leq (m(1-\mu))^{\alpha-1}$, the map f is defined via the branches $f_L(x)$ and $f_R(x)$ only:

$$f : x \mapsto \ f(x) = \begin{cases} f_L(x) = x^\alpha & \text{for } 0 \leq x \leq x_m, \\ f_R(x) = \widehat{x} & \text{for } x > x_m. \end{cases} \tag{7}$$

The boundary in the parameter space denoted BC and defined as

$$BC : \qquad \beta = (m(1-\mu))^{\alpha-1}, \tag{8}$$

is related to the appearance of the middle branch in the definition of f. Namely, for $\beta > (m(1-\mu))^{\alpha-1}$ the map f can be written in the following form:

$$f : x \mapsto \ f(x) = \begin{cases} f_L(x) = x^\alpha & \text{for } 0 \leq x \leq x_l, \\ f_M(x) = \left[\frac{1}{\mu\beta}\left(1 - \frac{x}{m}\right)\right]^{\alpha/(1-\alpha)} & \text{for } x_l < x \leq x_r, \\ f_R(x) = \widehat{x} & \text{for } x > x_r. \end{cases} \quad . \tag{9}$$

It is easy to see that besides the unstable fixed point in the origin related to the function $f_L(x)$, the map f has one more fixed point denoted x_i^*, $i \in \{L, M, R\}$, which can be associated with any one of the functions f_i, that is, satisfying $f_i(x_i^*) = x_i^*$, whose existence and stability properties are illustrated in Fig.s 1 and 2 described below.

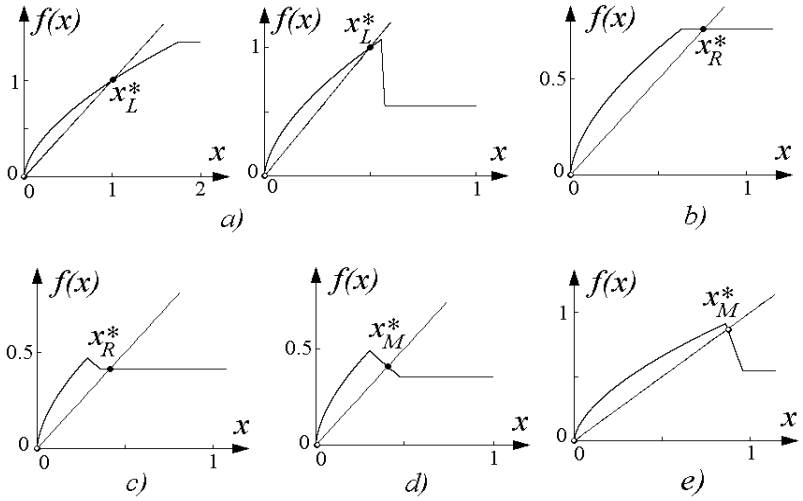

Figure 1: The map f and its fixed points at $\mu = 0.4$, $\beta = 0.8$ in *a)* on the left, $\mu = 0.05$, $\beta = 1.5$ in *a)* on the right (these parameter values belong to the region A, see Fig.2); *b)* $\mu = 0.7$, $\beta = 1.2$ (the region B); *c)* $\mu = 0.7$, $\beta = 1.8$ (the region C); *d)* $\mu = 0.6$, $\beta = 2$ (the region D); *e)* $\mu = 0.2$, $\beta = 1.5$ (the region E-I). The other parameter values are $m = 1.2$ and $\alpha = 0.6$.

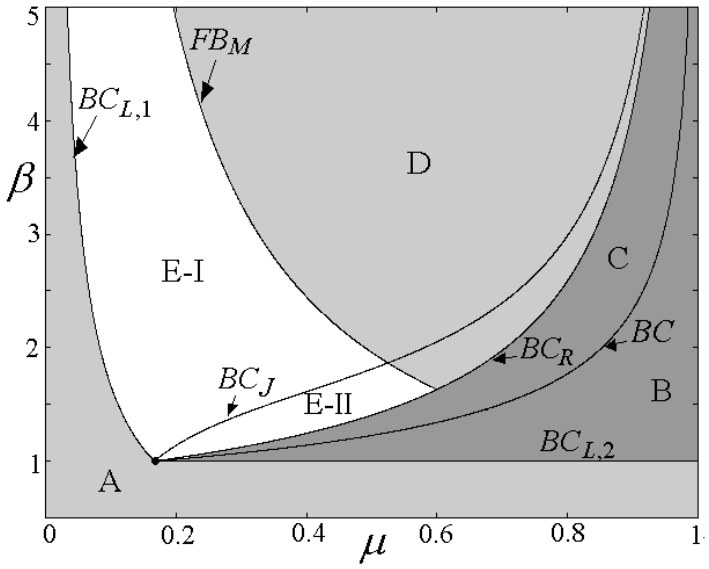

Figure 2: Partition of the (μ, β)-parameter plane at $m = 1.2$, $\alpha = 0.6$. The region A corresponds to the stable fixed point x_L^*; $B \cup C$ to the superstable fixed point x_R^*; D to the stable fixed point x_M^*; $E\text{-}I$ is related to the map f defined over the absorbing interval $J = [f^2(x_l), f(x_l)]$ by $f_L(x)$ and $f_M(x)$, and for $E\text{-}II$ in the absorbing interval $J = [f(x_r), f(x_l)$ the flat branch $f_R(x)$ is defined as well.

The second fixed point related to $f_L(x)$ is given by $x_L^* = 1$ (see Fig.1a). It exists for the parameter values belonging to the region denoted A in Fig. 2 and defined by

$$A: \qquad \beta \leq \max\left\{\frac{1}{\mu}\left(1 - \frac{1}{m}\right), 1\right\}. \tag{10}$$

The two boundaries of A correspond to the BCBs of x_L^* at which $x_L^* = x_c$, namely, if the parameter point belongs to the boundary

$$BC_{L,1}: \qquad \beta = \frac{1}{\mu}\left(1 - \frac{1}{m}\right), \tag{11}$$

we have $x_L^* = x_l$, and for

$$BC_{L,2}: \qquad \beta = 1, \tag{12}$$

we have $x_L^* = x_m$. If x_L^* exists, it is globally attracting. Note that in such a case we have $x_c \geq 1$, so that the map f in the interval $I = [0, 1]$ is defined by the branch $f_L(x)$ only.

The fixed point denoted x_R^* is related to the flat branch $f_R(x)$ and given by $x_R^* = \widehat{x}$. Clearly, $x_R^* < 1$, and x_R^* exists if $\widehat{x} \geq x_m$ (as in Fig.1b) or if $\widehat{x} \geq x_r$ (as in Fig.1c) that holds for the parameter region defined by

$$1 < \beta < (m(1-\mu))^{1-\frac{1}{\alpha}}. \tag{13}$$

If x_R^* exists it is a superstable fixed point, globally attracting. At the boundary $\beta = 1$ (denoted as $BC_{L,2}$ in (12)) $x_R^* = x_m$, moreover, $x_R^* = x_L^* = 1$. If the parameter point crosses $BC_{L,2}$ we observe the transition from the superstable fixed point x_R^* to the stable fixed point x_L^* (for example, see the transition from Fig.1b to Fig.1a (on the left)), so that it is the so-called *persistence border collision*.[1] While at the boundary

$$BC_R: \qquad \beta = (m(1-\mu))^{1-\frac{1}{\alpha}} \tag{14}$$

we have $x_R^* = x_r$, so that BC_R is related to one more border collision of x_R^*. The region of existence of x_R^* is divided by the boundary BC given in (8) in two subregions, denoted B and C in Fig.2:

$$B: \qquad 1 < \beta < (m(1-\mu))^{\alpha-1}, \tag{15}$$

$$C: \qquad (m(1-\mu))^{\alpha-1} < \beta < (m(1-\mu))^{1-\frac{1}{\alpha}}. \tag{16}$$

Finally, the fixed point x_M^* of the map f related to the middle branch $f_M(x)$ is implicitly defined by $x_M^* = \left[\frac{1}{\mu\beta}\left(1-\frac{x_M^*}{m}\right)\right]^{\alpha/(1-\alpha)}$ (see Fig.1d). It exists if $x_l \leq x_M^* \leq x_r$, and this is satisfied for parameter values belonging to the region defined by

$$\beta \geq \max\left\{\frac{1}{\mu}\left(1-\frac{1}{m}\right), (m(1-\mu))^{1-\frac{1}{\alpha}}\right\}. \tag{17}$$

Both boundaries of this region are related to the border collision of x_M^*, namely, at the boundary $BC_{L,1}$ (see (11)) we have $x_M^* = x_l$, moreover, $x_M^* = x_L^* = 1$, so that if the parameter point crosses $BC_{L,1}$ we observe the transition from the fixed point x_M^* to the stable fixed point x_L^* (for example, see the transition from Fig.1e to Fig.1a (on the right)). While at the boundary BC_R (see (14)) we have $x_M^* = x_r$, moreover, $x_M^* = x_R^*$ so that crossing BC_R we observe the transition from the superstable fixed point x_R^* to the fixed point x_M^* (see, for example, the transition from Fig.1d to Fig.1c). The slope of $f_M(x)$ at the fixed point x_M^* is negative, so that it may become unstable via a flip bifurcation (which is subcritical for $\alpha < 0.5$, degenerate for $\alpha = 0.5$ and supercritical for $\alpha > 0.5$). The flip bifurcation curve of x_M^* is given by

$$FB_M: \qquad \beta = \frac{\alpha}{\mu}(m(1-\alpha))^{1-\frac{1}{\alpha}}. \tag{18}$$

[1] Recall that *persistence border collision* of a fixed point occurs when the fixed point crosses the border without changing its stability.

Thus for parameter values belonging to the region denoted D defined by

$$D: \qquad \beta > \max\left\{\frac{\alpha}{\mu}(m(1-\alpha))^{1-\frac{1}{\alpha}}, (m(1-\mu))^{1-\frac{1}{\alpha}}\right\}$$

(see Fig.2) there exists the locally attracting fixed point x_M^*.

Let us define now an *invariant absorbing interval* of the map f given in (9), denoted J. By definition of invariance we must have $f(J) = J$, while the property to be absorbing means that any orbit of f enters J in a finite number of iterations (and stays there forever). Moreover, J has to be bounded either by two critical points or by a critical point and its image. For the map f there are two possibilities:

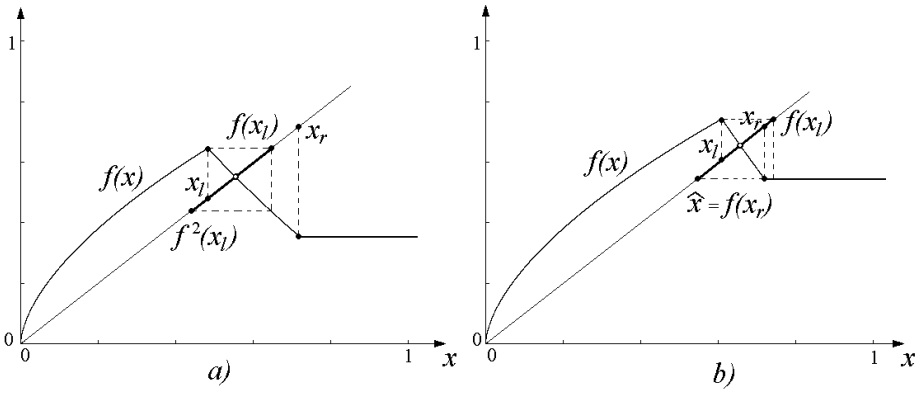

Figure 3: The invariant absorbing interval $J = [f^2(x_l), f(x_l)]$ in *a)* and $J = [f(x_r), f(x_l)]$ in *b)* of the map f for the parameter values belonging to the regions *E-I* and *E-II*, respectively. Here $m = 1.2$, $\alpha = 0.6$ $\mu = 0.4$ and $\beta = 2$ in *a)*, $\beta = 1.5$ in *b)*.

(1) In the absorbing interval J only the functions $f_L(x)$ and $f_M(x)$ are defined, that holds for parameter values belonging to the region denoted *E-I* in Fig.2 defined as

$$E\text{-}I: \left\{ \begin{array}{l} \beta < \frac{\alpha}{\mu}(m(1-\alpha))^{1-\frac{1}{\alpha}}, \\ \beta > \max\left\{\frac{1}{\mu}\left(1-\frac{1}{m}\right),\ 1-\frac{1}{\mu}+\frac{1}{\mu}(m(1-\mu))^{1-\frac{1}{\alpha}}\right\}. \end{array} \right. \tag{19}$$

In such a case $J = [f^2(x_l), f(x_l)]$ (an example is shown in Fig.3*a*).

(2) All the three functions, $f_L(x)$, $f_M(x)$ and $f_R(x)$, are involved in J, that holds in the region denoted *E-II* in Fig.2 given by

$$E\text{-}II: \left\{ \begin{array}{l} \beta > (m(1-\mu))^{1-\frac{1}{\alpha}}, \\ \beta < \min\left\{1-\frac{1}{\mu}+\frac{1}{\mu}(m(1-\mu))^{1-\frac{1}{\alpha}},\ \frac{\alpha}{\mu}(m(1-\alpha))^{1-\frac{1}{\alpha}}\right\}. \end{array} \right. \tag{20}$$

In such a case $J = [f(x_r), f(x_l)] = [\widehat{x}, f(x_l)]$ (see Fig.3b for an example). The contact of J with the border point x_r, occurring when the condition $f(x_l) = x_r$ is satisfied, corresponds to the boundary

$$BC_J : \qquad \beta = 1 - \frac{1}{\mu} + \frac{1}{\mu}(m(1-\mu))^{1-\frac{1}{\alpha}}. \tag{21}$$

Preliminary description of the bifurcation structure of the region E-I defined in (19) is discussed in [27], and it is a subject of the forthcoming paper. The main object of the present paper is the bifurcation structure of the region E-II given in (20), formed by the periodicity regions related to superstable cycles of the map f existing due to its flat branch. From now on we shall consider the parameter values belonging to the region E-II.

To distinguish between different cycles with the same period it is quite convenient to use their symbolic representation. To write down the *symbolic sequence* of an n-cycle $\gamma_n = \{x_i\}_{i=1}^n$ of the map f given in (9) we need at most 5 symbols: the symbol L is used for the periodic points $x_i : 0 < x_i < x_l$, the symbol M is reserved for $x_i : x_l < x_i < x_r$, the symbol R is used for $x_i : x_i > x_r$, and the symbols C_l and C_r are used for $x_i = x_l$ and $x_i = x_r$, respectively. In such a way the symbolic sequence, denoted σ, of the cycle γ_n consists of n symbols related to the location of the periodic points: $\sigma = \sigma_1\sigma_2...\sigma_n$, $\sigma_i \in \{L, C_l, M, C_r, R\}$.

Let γ_n be a superstable cycle of the map f, and let $x_1 > x_r$, so that the first symbol of the symbolic sequence of γ_n is R (given that any cycle can have at most one point in the definition region of f_R, the symbolic sequence of such a cycle has only one symbol R). Then $x_2 = f_R(x_1) = \widehat{x}$, that is, any superstable cycle of the map f consists of the point $\widehat{x}$ and its $n-1$ images by f. Obviously, two superstable cycles cannot coexist, while coexistence of a superstable cycle and a stable cycle (with symbolic sequence consisting of symbols L and M only) is possible, as well as coexistence of two stable cycles. The *basin of attraction* of any superstable cycle γ_n denoted $\mathcal{S}$ is given by the interval $[x_r, \infty)$ related to the flat branch, and the preimages of any rank $i > 0$ of the interval $[x_r, f_L(x_l)]$:

$$\mathcal{S} = \cup_{i=1}^{\infty} f^{-i}([x_r, f_L(x_l)]) \cup [x_r, \infty). \tag{22}$$

Obviously, any point of $\mathcal{S}$ is preperiodic to γ_n, that is, it is mapped into γ_n in a finite number of iterations. Note that due to noninvertibility of f, its inverse function is not uniquely defined, so that constructing the set $\mathcal{S}$ one has to include all the preimages of the interval $[x_r, f_L(x_l)]$ by all the three branches of the inverse function. See, for example, Fig.4 which shows the map f, its superstable 3-cycle $\gamma_3 = \{f_L^2(\widehat{x}), \widehat{x}, f_L(\widehat{x})\}$ with the symbolic sequence RL^2, and the interval $[x_r, f_L(x_l)]$ together with a few its preimages. In this case the set of preimages of any rank fills densely the absorbing interval $J = [\widehat{x}, f(x_l)]$. However, it is clear that not all the points of J are mapped into γ_3. There exist an invariant set of points which are not mapped into the cycle γ_3 defining its basin boundary, which is a chaotic repeller (of zero Lebesgue measure) consisting of the points of all the repelling cycles, their preimages of any rank and an uncountable set of aperiodic orbits. Indeed, it can be shown that for any superstable cycle γ_n

its basin boundary has such a complicated structure, except for the superstable 2-cycle and its harmonics (that is, the 2^k-cycles, $k > 1$, born due to a cascade of flip BCBs of the 2-cycle) as we clarify in next sections.

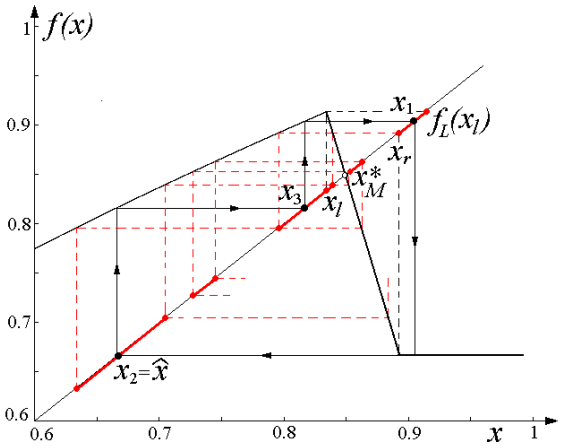

Figure 4: The map f and its superstable cycle $\gamma_3 = \{x_i\}_{i=1}^3$. The interval $[x_r, f_L(x_l)]$ and several of its preimages are shown in red. Here $m = 1.05$, $B = 1.5$, $\alpha = 0.5$ and $\mu = 0.15$.

3 Numerical results

In this section we present numerical results illustrating the bifurcation structure of the region E-II in the parameter space of the map f, related to its *superstable cycles*.

The 2D bifurcation diagram in the (μ, β)-parameter plane for $m = 1.2$, $\alpha = 0.6$ is shown in Fig.5a, and for $m = 1.2$, $\alpha = 0.5$ in Fig.5b. Fig.6 presents the 2D bifurcation diagram in the (μ, α)-parameter plane and its enlargement for $m = 1.05$, $B = 1.5$. In these figures different colors correspond to the periodicity regions related to attracting cycles of periods $n \leq 30$ (the correspondence of the colors and periods is indicated at the color bar), and white color is related to either higher periodicity regions or to chaotic attractors. Note that several regions of the same color are related to attracting cycles having the same period but different symbolic sequences, for example, in Fig.6b three 5-periodicity regions are clearly visible. As we shown in the next section, the rightmost 5-periodicity region is related to the superstable cycles with symbolic sequences RLM^3 and RLM^2L, the middle region to RL^2ML and RL^2M^2 and the left region to RL^3M and RL. The bifurcation curves $BC_{L,1}$, $BC_{L,2}$, BC_R, FB_M as well as the curves BC and BC_J are plotted using their analytical expressions derived in the previous section (note that the boundary $BC_{L,2}$ in Fig.6 is defined

by $\alpha = 0.6$, obtained from $\beta = B\frac{1-\alpha}{\alpha}$ at $\beta = 1$ and $B = 1.5$). Some periodicity regions are additionally marked by the corresponding periods.

As we have already mentioned, two superstable cycles of the map f cannot coexist, while a superstable cycle can coexist with a stable cycle. In Fig.s 5 and 6 the regions related to coexisting attractors cannot be seen (except for the narrow green region bounded from above by the subcritical flip bifurcation curve FB_M in Fig. 6*a,* related to coexisting attracting fixed point x^*_M and 2-cycle), because only one initial condition has been used to plot these diagrams. The problem of coexistence of different attractors is discussed in the forthcoming paper.

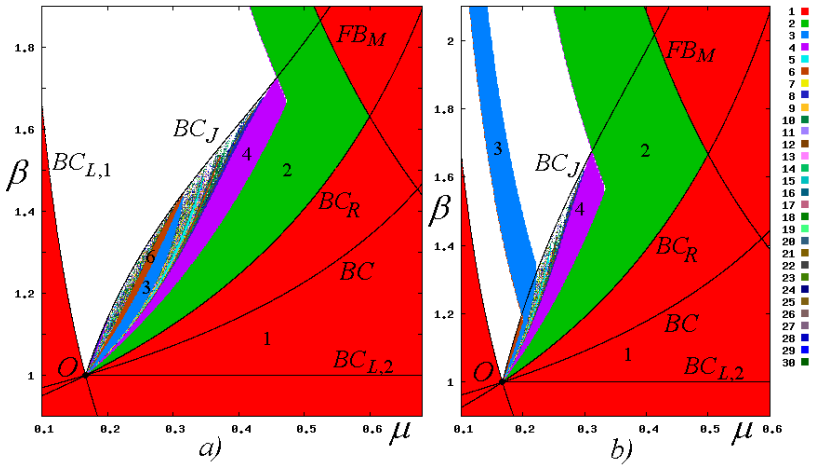

Figure 5: 2D bifurcation diagram of the map f in the (μ, β)-paramter plane at $m = 1.2$ and $\alpha = 0.6$ in *a)*, $\alpha = 0.5$ in *b)*.

A first observation is related to the particular bifurcation point denoted O in Fig.s 5 and 6, which is the intersection point of several border collision curves, namely, $BC_{L,1}$, $BC_{L,2}$ and BC_R. However, it can be clearly seen that not only these bifurcation curves issue from O, but also infinitely many curves bounding periodicity regions which belong to the region $E\text{-}II$. Following the notation in [1], the codimension-2 bifurcation point O is called *organizing center*, defined as a bifurcation point from which an infinite number of codimension-1 bifurcation curves issue.

Let P_σ denote the periodicity region related to the cycle with the symbolic sequence σ. We first clarify which bifurcations define the boundaries of the regions P_σ using as an example the 3-periodicity region (see Fig.6*b*). This region consists of three subregions, namely, the regions P_{RLM} and P_{RL^2} related to the superstable 3-cycles with the symbolic sequences RLM and RL^2, respectively, and the region P_{ML^2} related to the stable 3-cycle with the symbolic sequence ML^2. Note that even if a part of the region P_{ML^2} belongs to the region $E\text{-}II$,

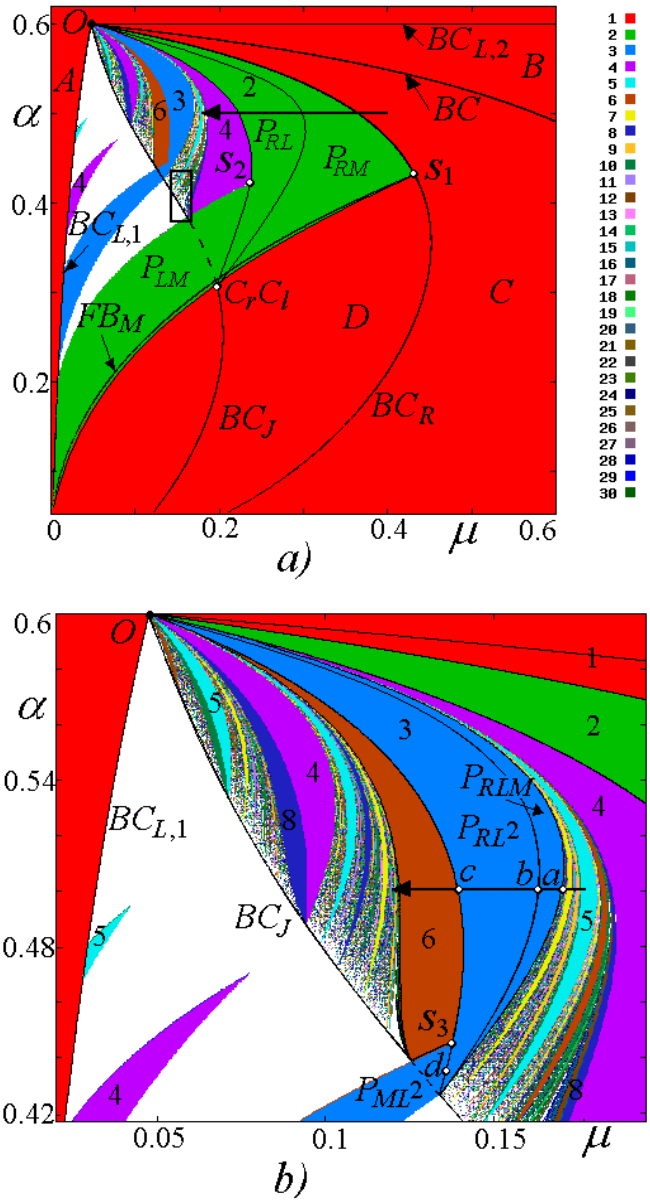

Figure 6: 2D bifurcation diagram of the map f in the (μ, α)-parameter plane at $m = 1.05$, $B = 1.5$ in *a)* and its enlargment in *b)*. The rectangle marked in *a)* is shown enlarged in Fig.13.

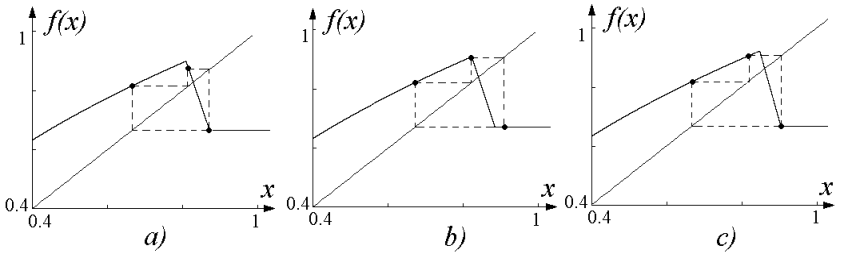

Figure 7: The 3-cycle γ_3 at the moment of the border collision: in *a)* γ_3 has the symbolic sequence C_rLM, in *b)* γ_3 is represented by RLC_l and in *c)* γ_3 has the symbolic sequence C_rL^2. Here $m = 1.05$, $B = 1.5$, $\alpha = 0.5$ and $\mu = 0.17$ in *a)*, $\mu = 0.1638$ in *b)*, $\mu = 0.1394$ in *c)* (the related parameter points are marked a, b and c, resp., in Fig.6*b*).

for which the absorbing interval involves all the three branches of f, the stable 3-cycle ML^2 is defined by the functions f_L and f_M only.[2] The boundaries of the regions P_{RL^2} and P_{RLM} shown in Fig.6*b* are plotted using the conditions of the border collision of the related 3-cycle. Namely, the right boundary of P_{RLM} denoted BC_{C_rLM} is related to the 3-cycle C_rLM as, for example, the cycle shown in Fig.7*a* (the related parameter point is marked a in Fig.6*b*); the left boundary BC_{RLC_l} of P_{RLM}, which is also the right boundary of P_{RL^2}, is related to the 3-cycle RLC_l, as, for example, the one shown in Fig.7*b* (the related parameter point is marked b in Fig.6*b*) and the left boundary $BC_{C_rL^2}$ of P_{RL^2} corresponds to the 3-cycle C_rL^2, as in Fig.7*c* (the related parameter point is marked c in Fig.6*b*). Note that all the three curves BC_{C_rLM}, BC_{RLC_l} and $BC_{C_rL^2}$ issue from the point belonging to the curve BC_J and related to the 3-cycle C_rLC_l.

In a similar way we can obtain the boundaries of the 2-periodicity region shown in green in Fig.6*a,* consisting of three subregions, namely, the regions P_{RM}, P_{RL} and P_{LM}. The lower boundary of P_{RM} (connecting the points marked s_1 and C_lC_r) is related to the 2-cycle C_rM hence denoted as BC_{C_rM}, the right boundary of P_{RM} (connecting s_1 and O) is just the curve BC_R, and its left boundary which is also the right boundary of P_{RL} (connecting C_lC_r and O), corresponds to 2-cycle RC_l, hence denoted as BC_{RC_l}. The left boundary of P_{RL} is related to the cycle C_rL, hence denoted as BC_{C_rL}. The narrow region bounded by the curves BC_{C_rM}, BC_{RC_l} and FB_M (note that $\alpha < 0.5$ here, thus, the flip bifurcation is subcritical) is related to coexisting stable fixed point x^*_M and superstable 2-cycle RM, while the region bounded by BC_{RC_l}, BC_{C_rL} and FB_M is related to the coexistence of the stable fixed point x^*_M and the superstable 2-cycle LR. This bifurcation structure is schematically illustrated

[2] The region P_{ML} seen in Fig.6*a* and the region P_{ML^2} seen in Fig.6*b* belong to both regions *E-I* and *E-II*. For different values of m other periodicity regions, related to stable but not superstable cycles, belonging to *E-I* can extend to *E-II* as well.

in Fig.8a where the bistability regions mentioned above, as well as the region of coexistence of the stable fixed point x_M^* and the stable 2-cycle LM, are dashed. Additionally it is indicated that stable 2-cycles with symbolic sequences LM^s, RL^s and RM^s (the index s means stability) born due the fold BCB in pair with the unstable cycle MM^u (the index u means that this cycle is unstable) coexist with the stable fixed point x_M^* indicated by the symbol M^s. If the parameter point crosses the curve FB_M the fixed point M^s and the unstable 2-cycle MM^u merge, the fixed point losses stability, the 2-cycle MM^u disappears, so that above the curve FB_M there exist the unstable fixed point x_M^* and the related 2-cycle (stable or superstable). Such a bifurcation structure is observed in the (μ, α)-parameter plane if $\alpha < 0.5$ at the point s_1 and, thus, the flip bifurcation is subcritical (as, for example, it occurs in Fig.6a). The bifurcation structure in the case of a supercritical flip bifurcation of x_M^* is schematically illustrated in Fig.8b for $\alpha > 0.5$ at the point C_rC_l. Note that it is possible to have $\alpha < 0.5$ at C_rC_l and $\alpha > 0.5$ at s_1, in which case FB_M intersects with BC_{C_rM}, and it is also possible that the curve FB_M intersects with the curve BC_{C_lM} (for $\alpha > 0.5$ at C_rC_l). In both cases we have $\alpha = 0.5$ at the intersection point, and the flip bifurcation is supercritical above the intersection and subcritical below it.

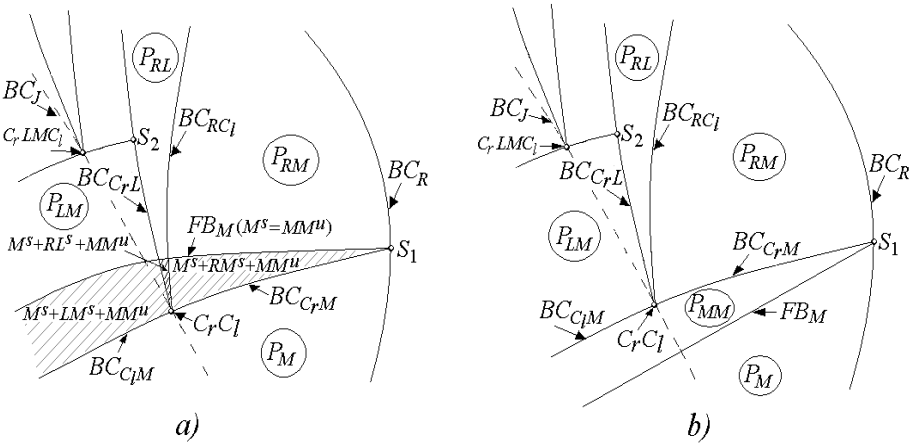

Figure 8: Schematic structure of the regions P_{RM}, P_{RL} and P_{LM} in the (μ, α)-parameter plane. With $\alpha < 0.5$ at s_1, a) shows the case of a subcritical flip bifurcation of x_M^* with the bistability regions dashed; with $\alpha > 0.5$ at C_rC_l b) shows the case of supercritical flip bifurcation of x_M^*.

To see what kind of bifurcation occurs when parameter point crosses boundaries of a periodicity region related to superstable n-cycle, recall first that the only bifurcation which is possible for a superstable cycle, is a BCB. Using the skew tent map as the BCB normal form (see, e.g., [35]), it is easy to show that a superstable n-cycle γ_n can undergo either a fold BCB or a flip BCB or a per-

sistence border collision. In fact, evaluating the left- and right-side derivatives, denoted a and b, of the function f^n at the border-crossing superstable fixed point of f^n at the bifurcation parameter value, we have that one such derivative is obviously 0, say, $a = 0$, and, depending on the other derivative, b, the following cases can be distinguished:

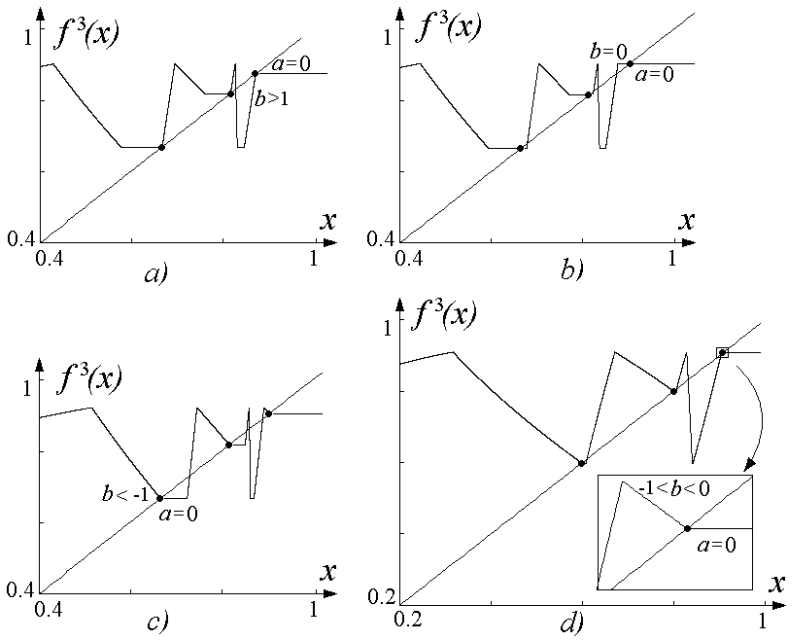

Figure 9: The map f^3 and its border-crossing fixed points related to the 3-cycle of the map f. Here the parameter values in *a)*, *b)*, *c)* are as in Fig.7, and $\alpha = 0.435$, $\mu = 0.1358$ in *d)* (the related parameter points are indicated by a, b, c and d, resp., in Fig.6b).

(1) if $b > 1$ then a *fold BCB* (also referred to as *nonsmooth fold bifurcation*) occurs at which one point of γ_n and one point of the repelling complementary[3] n-cycle collide with the border point simultaneously and both cycles disappear after the bifurcation (an example of f^3 together with the border-crossing fixed points at the moment of the fold BCB is shown in Fig.9a; the related parameter point is marked by a in Fig.6b);

(2) if $|b| < 1$, then a *persistence border collision* occurs at which the superstable cycle γ_n is transformed into the complementary cycle which is either again superstable, or stable (see Fig.s 9b and 9d, respectively; the related parameter points are marked by b and d in Fig.6b).

[3]Two cycles of a continuous piecewise smooth map, born at a *fold BCB* are so-called *complementary* cycles: their symbolic sequences differ by the one, colliding, symbol.

(3) if $b < -1$ then a supercritical *flip BCB* occurs at which γ_n is transformed into the complementary repelling n-cycle, while a superstable $2n$-cycle γ_{2n} is born (see Fig.9c and the related parameter point marked by c in Fig.6b).

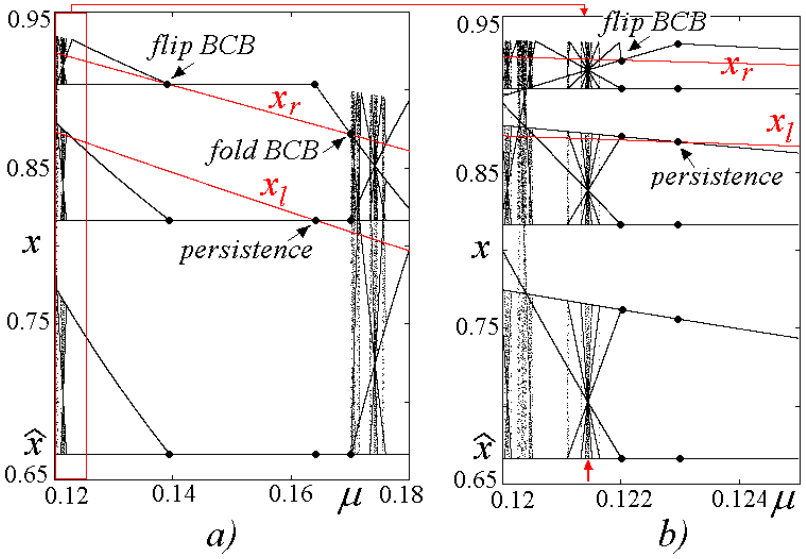

Figure 10: 1D bifurcation diagram of the map f at $m = 1.05$, $B = 1.5$, $\alpha = 0.5$ and $\mu \in [0.12, 0.18]$ in *a)* (the related parameter path is indicated in Fig.6b by the horizontal line with an arrow), and $\mu \in [0.12, 0.125]$ in *b)*, which is the enlarged window indicated in *a)*.

The results of these bifurcations are illustrated in the 1D bifurcation diagram shown in Fig.10a, corresponding to the parameter path for fixed $\alpha = 0.5$ varying μ, as indicated in Fig.6b by the horizontal line with an arrow. In particular, it can be seen that at $\mu \approx 0.17$ the boundary BC_{C_rLM} is crossed (see the point a in Fig.6b) and the fold BCB occurs at which for decreasing μ the superstable cycle RLM is born together with the complementary repelling cycle MLM (which is not shown). At the moment of the fold BCB these cycles coincide and have the symbolic sequence C_rLM (see also Fig.7a). At $\mu \approx 0.1638$ the parameter point crosses the boundary BC_{RLC_l} (see the point b in Fig.6b) and the persistence border collision occurs: the cycle RLM is transformed into the cycle RL^2 (the persistence border collision occurs also if the boundary $BC_{C_rL^2}$ is crossed below the point marked by s_3 in Fig.6b, e.g., at the point d, in which case we observe the transition from RL^2 to ML^2). At $\mu \approx 0.1394$ the boundary $BC_{C_rL^2}$ is crossed (see the point c in Fig.6b) and the flip BCB occurs leading to the superstable 6-cycle with the symbolic sequence RL^2ML^2.

Fig.10b shows an enlargement of the window indicated in Fig.10a, where it can be seen that the superstable 6-cycle RL^2ML^2 for decreasing μ first undergoes the persistence border collision, at $\mu \approx 0.123$, being transformed into the

superstable cycle RL^2MLM. Both the sequences RL^2ML^2 and RL^2MLM are the so-called *first harmonics* of RL^2, as explained in the next section. We continue to decrease the value of μ, and at $\mu \approx 0.122$ the flip BCB occurs, leading to the superstable 12-cycle with the symbolic sequence $RL^2MLM^2L^2MLM$. The 12-cycle in its turn also first undergoes the persistence border collision, at $\mu \approx 0.12197$, leading to the cycle $RL^2MLM^2L^2ML^2$ (both $RL^2MLM^2L^2MLM$ and $RL^2MLM^2L^2ML^2$ are the *second harmonics* of RL^2), which then, at $\mu \approx 0.1216$, undergoes the flip BCB resulting to the 24-cycle whose symbolic sequence $RL^2MLM^2L^2ML^2ML^2MLM^2L^2ML^2$ (the *third harmonic* of RL^2). Indeed, an infinite cascade of flip BCBs occurs for decreasing μ which is difficult to observe numerically due to the high rate of the compression of the related parameter ranges. The sequence of superstable cycles described above can be written schematically as follows:

$$... \overset{C_rLM}{\rightarrow} RLM \overset{RLC_l}{\rightarrow} RL^2 \overset{C_rL^2}{\rightarrow} RL^2ML^2 \overset{RL^2MLC_l}{\rightarrow} RL^2MLM \overset{C_rL^2MLM}{\rightarrow} RL^2MLM^2L^2MLM...$$

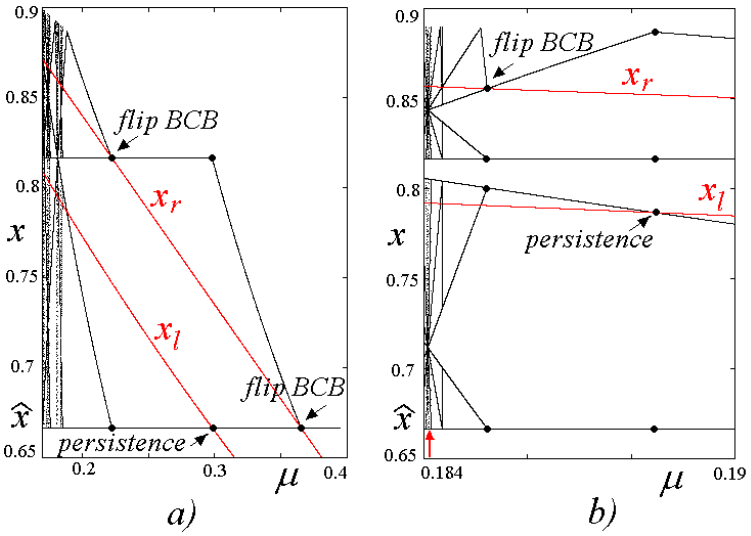

Figure 11: 1D bifurcation diagram of the map f at $m = 1.05$, $B = 1.5$, $\alpha = 0.5$, and $\mu \in [0.175, 0.4]$ in *a)* (the related parameter path is indicated in Fig.6*a* by the horizontal line with an arrow); $\mu \in [0.184, 0.19]$ in *b)* (it is an enlargment of *a)*).

As one more example, let us consider the cascade of flip BCBs of the 2-cycle. It is illustrated in Fig.11 by means of the 1D bifurcation diagram (the related parameter path for fixed $\alpha = 0.5$ and varying μ is indicated by the

horizontal line with an arrow in Fig.6a). Namely, the following sequence of flip BCBs (related to the collision with the border point x_r) and persistence border collisions (due to the collision with the border point x_l) can be observed for decreasing μ. The superstable fixed point x_R^* whose symbolic sequence is just one symbol R, undergoes the flip BCB (the parameter point crosses the boundary BC_R above the point s_1, see Fig.6a), that leads to a 2-cycle with symbolic sequence RM. Then this cycle is transformed into the one with symbolic sequence RL due to the persistence border collision (the parameter point crosses the boundary BC_{RC_L}). Note that the sequences RM and RL are the first harmonics of R. Then the 2-cycle RL undergoes the flip BCB (the parameter point crosses the boundary BC_{C_rL} above the point s_2) leading to a 2^2-cycle whose symbolic sequence is $RLML$. Then this cycle changes its symbolic sequence to RLM^2 due to persistence border collision ($RLML$ and RLM^2 are the second harmonics of R). Then it undergoes the flip BCB leading to a 2^3-cycle with the symbolic sequence RLM^3LM^2 which is transformed into RLM^3LML due to the persistence border collision (RLM^3LM^2 and RLM^3LML are the third harmonics of R), so on, as schematically represented as follows:

$$R \overset{C_r}{\to} RM \overset{RC_l}{\to} RL \overset{C_rL}{\to} RLML \overset{RLMC_l}{\to} RLM^2 \overset{C_rLM^2}{\to} RLM^3LM^2... \qquad (23)$$

As we have mentioned in the previous section, in the case of the superstable 2-cycle RL or any of its harmonics, the basin of attraction defined in (22) has a simpler structure than in the generic case, being not associated with a chaotic repeller on the basin boundary. For example, it is easy to see that in case of the 2-cycle RL shown in Fig.12a, any point of the absorbing interval $J = [\widehat{x}, f(x_l)]$, except for the unstable fixed point x_M^*, is mapped into this cycle in a finite number of iterations while in case of the 4-cycle RLM^2 shown in Fig.12b, any point of J is mapped into this cycle except for the unstable fixed point x_M^*, unstable 2-cycle LM and its preimages (converging in backward iterations by f_M^{-1} to x_M^*). In general, for a superstable cycle whose symbolic sequence is the k-th harmonic of R, $k > 0$, the basin boundary includes the fixed point x_M^*, the points of all the m-harmonic cycles for any $m < k$ (which are unstable due to flip BCBs), as well as their preimages. Such a structure of the basin boundary is qualitatively similar to the one of an attracting 2^k-cycle of the logistic map born during the first cascade of period-doubling bifurcations.

Let us now consider the sets in the parameter space to which the periodicity regions of the superstable cycles are accumulating, and the dynamics related to these sets. Such accumulation parameter values are visible in the 1D bifurcation diagrams as those related to the "bodies of the spiders", like, for example, the value $\mu = 0.1215$ indicated by a red arrow in Fig.10b. For the logistic map it is known that the periodicity windows at the well-known 1D bifurcation diagram are accumulating to the parameter values related to homoclinic bifurcations of the unstable cycles. Moreover, on the other side of any accumulation point of a cascade of period-doubling bifurcations, a cascade of the homoclinic bifurcations is accumulating. To see that for the map f the periodicity regions are accumulating on the parameter sets related to homoclinic bifurcations of the

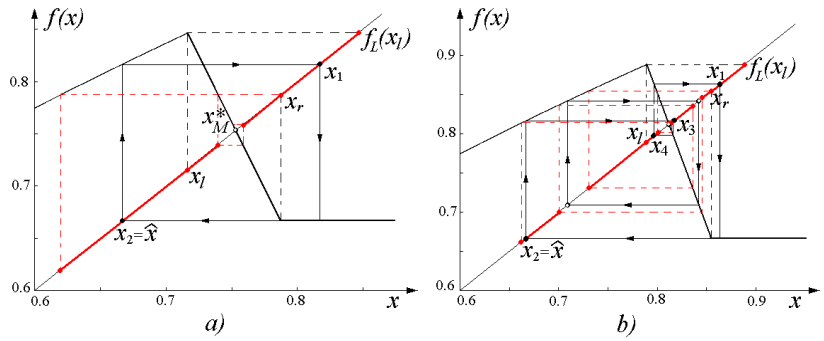

Figure 12: In *a)* the cycle $\gamma_2 = \{x_i\}_{i=1}^2$ and in *b)* the cycle $\gamma_4 = \{x_i\}_{i=1}^4$ which is the first harmonic of γ_2, are shown. Any point of $J = [\widehat{x}, f(x_l)]$ is mapped into the attractor except for x_M^* in *a),* and except for x_M^*, the 2-cycle LM (shown by white circles) and its preimages in *b).* Here $m = 1.05$, $B = 1.5$, $\alpha = 0.5$ and $\mu = 0.25$ in *a)*, $\mu = 0.186$ in *b).*

corresponding cycles, we first present in Fig.13 the enlargement of the window marked by the rectangle in Fig.6*a,* and in Fig.14 the 1D bifurcation diagram related to the parameter path indicated in Fig.13 by the horizontal line with an arrow which pierces the red circle on the line H_2. In this diagram the accumulation points $\mu = \mu_{H_1}$ and $\mu = \mu_{H_2}$ are clearly visible, related to the first homoclinic bifurcations of the fixed point x_M^* and of the 2-cycle with the symbolic sequence LM, respectively.

Let us first consider the 2-cycle with the symbolic sequence LM, that is, the cycle $\gamma_2 = \{x_1, x_2\}$ where $x_1 < x_l$, $x_l < x_2 < x_r$, $f_L(x_1) = x_2$ and $f_M(x_2) = x_1$. Its first homoclinic bifurcation is defined by the condition of the border point x_l to be preperiodic to this cycle, namely, as illustrated in Fig.15, this condition can be written as

$$f_M \circ f_M \circ f_L \circ f_R \circ f_L(x_l) = x_2, \tag{24}$$

or, taking into account that for the parameter region $E\text{-}II$ we have $f_R \circ f_L(x_l) = f_R(x_r)$, the condition in (24) becomes

$$f_M \circ f_M \circ f_L \circ f_R(x_r) = x_2,$$

or also, considering that $f_R(x) = \widehat{x}$, we have:

$$f_M \circ f_M \circ f_L(\widehat{x}) = x_2. \tag{25}$$

The bifurcation curve numerically obtained corresponding to the condition in (25) is denoted H_2 in Fig.13. In Fig.15 we present the map f at the moment of the first homoclinic bifurcation of the 2-cycle (the related point of the curve H_2 is marked by red circle in Fig.13). It can be seen that even if this cycle is locally repelling almost all the points of the absorbing interval $J = [\widehat{x}, f(x_l)]$ are

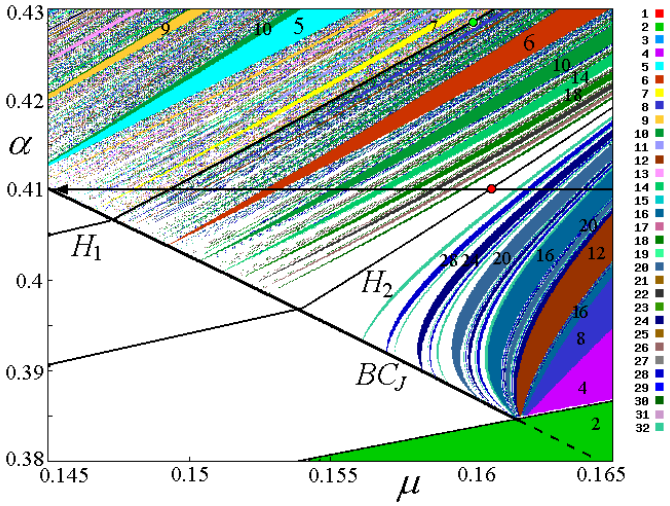

Figure 13: An enlargment of the window indicated in Fig.6a by the rectangle. The curves marked H_1 and H_2 are related to the first homoclinic bifurcations of the fixed point x^*_M and 2-cycle with the symbolic sequence LM, resp.

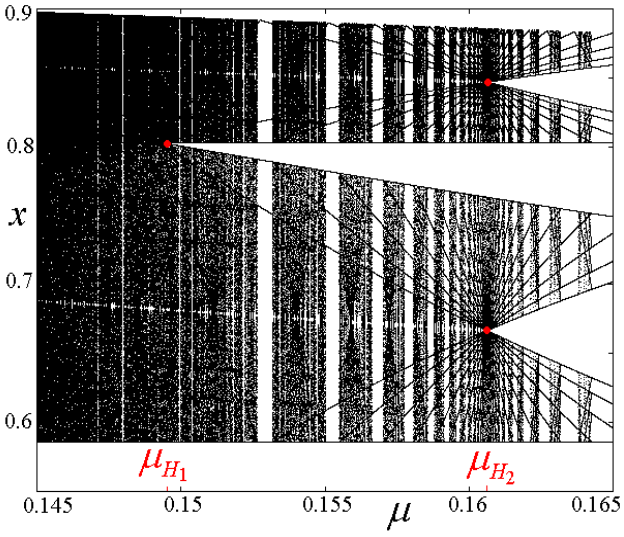

Figure 14: 1D bifurcation diagram of the map f at $m = 1.05$, $B = 1.5$, $\alpha = 0.41$ and $\mu \in [0.145, 0.165]$ (the related parameter path is indicated in Fig.13 by the horizontal line with an arrow). The values $\mu = \mu_{H_1}$ and $\mu = \mu_{H_2}$ correspond to the first homoclinic bifurcations of the fixed point and 2-cycle, resp.

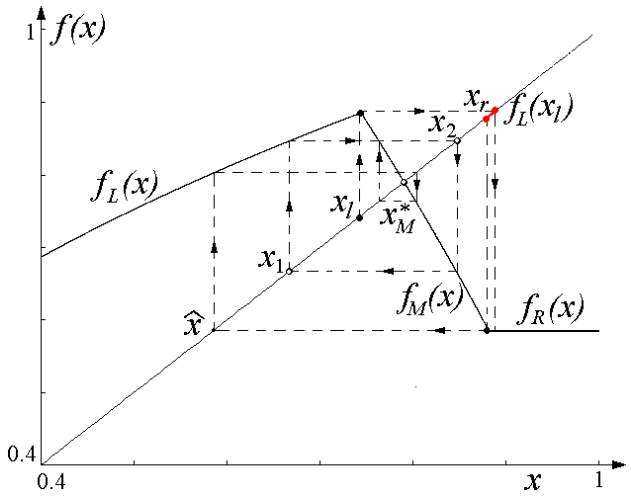

Figure 15: The map f for the parameter values corresponding to the first homoclinic bifurcation of the 2-cycle $\gamma_2 = \{x_1, x_2\}$. Here $m = 1.05$, $B = 1.5$, $\alpha = 0.41$ and $\mu = 0.160635 \approx \mu_{H_2}$. The related parameter point belongs to the curve H_2 and is marked by the red circle in Fig.13.

mapped into this cycle, so it is an attractor in Milnor sense[4]. This occurs due to the flat branch f_R, namely, the complete interval $[x_r, \infty)$ is ultimately mapped to the point x_2, as well as infinitely many preimages of the interval $[x_r, f_L(x_l)]$ marked by red in Fig.15. Its preimages of increasing rank fill densely the interval J and define the stable set, given in (22), of the locally repelling 2-cycle γ_2. We notice that any homoclinic cycle of the map f for the considered parameter range has the stable set as given in (22). Clearly in J there exist also infinitely many points which are not attracted to the cycle γ_2, which belong to the chaotic repeller of zero Lebesgue measure consisting of the points of all the repelling cycles, their preimages of any rank and their limit sets.

One more example is shown in Fig.16 where the function f is plotted at the parameter values corresponding to the first homoclinic bifurcation of the fixed point x^*_M (the related parameter point belongs to the curve H_1 and marked by green circle in Fig.13), which in our case also leads to an attractor in Milnor sense, whose stable set is as given in (22). A few preimages of the interval $[x_r, f_L(x_l)]$ are shown in red in Fig.16 and all the existing preimages are filling densely the interval J. The condition of the first homoclinic bifurcation of x^*_M

[4] Denoting by $\omega(x)$ the set of accumulation points of the orbit under the forward iterations of x, called ω-limit set of x, we recall that a *Milnor attractor* is defined as a closed invariant set $A \subset J$ such that the set $\rho(A)$ consisting all the points $x \in J$ for which $\omega(x) \subset A$ has *strictly positive* measure, and there is no strictly smaller closed subset A' of A such that $\rho(A')$ coincides with $\rho(A)$ up to a set of measure zero [29].

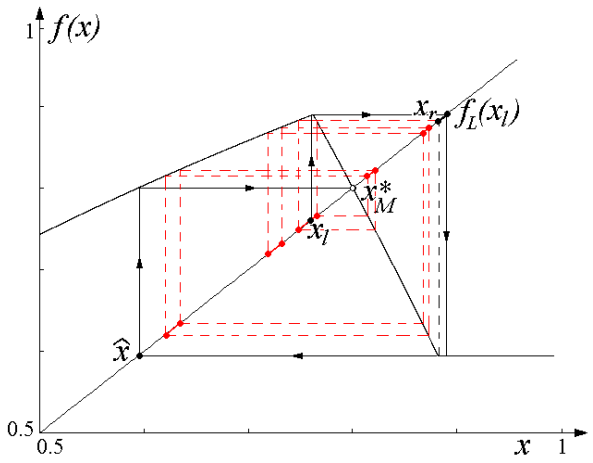

Figure 16: The function f for the parameter values related to the first homoclinic bifurcation of the fixed point M. Here $m = 1.05$, $B = 1.5$, $\mu = 0.16$, $\alpha = 0.4285$. This parameter point belongs to the curve H_1 and marked by the green circle in Fig.13.

is given by

$$f_L \circ f_R(x_r) = x^*_M, \tag{26}$$

where we recall that the fixed point x^*_M is implicitly defined from $x^*_M = f_M(x^*_M)$. The bifurcation curve related to the condition in (26) is denoted H_1 in Fig.13.

4 Modified U-sequence

The numerical results presented in the previous section suggest that the periodicity regions of the superstable cycles of the map f given in (9) are ordered according to the well-known U-sequence. Recall that the U-sequence (where "U" stands for "universal") was first described in [28] and referred to symbolic sequences of *superstable* cycles of maps of a particular class. Namely, it was established for 1D continuous piecewise differentiable maps $g : I \to I$ depending on a parameter, with a unique maximum $g_{\max}$ assumed either at a point or in an interval, and such that to the left or right of this point (or interval) the map is strictly increasing or strictly decreasing, respectively. Additionally it was assumed that at any x such that $g(x) = g_{\max}$ the derivative of g exists and is equal to 0, and the condition defining the parameter range. The most known example of maps whose superstable cycles are ordered on parameter according to the U-sequence are unimodal maps[5] with "smooth" maximum, in which case

[5] A 1D continuous map $g : I \to I$ is called *unimodal* if there exists exactly one point of local extrema in the interior of I, moreover, g is strictly increasing on one side of the point of local extrema and strictly decreasing on the other side.

the U-sequence can be easily extended to the sequence of *stable* cycles (as we clarify below using the logistic map as an example). However, in [28] it was also mentioned, that the conditions listed above are sufficient to guarantee the existence of the U-sequence, but not necessary. In fact, it is known (see, e.g., [17]) that the U-sequence is valid also for the unimodal maps which are not differentiable at the point of maximum (as, for example, the considered map f for parameter values belonging to the region E-I given in (19), or the skew tent map), in which case the U-sequence may be related to not only stable but also *unstable* cycles, or even unstable cycles only (in [28] the U-sequence in the tent map was mentioned as an example of such a case). Obviously, the considered map f for parameter values belonging to the region E-II given in (20) does not belong to the classes of maps mentioned above. To see why the U-sequence is nevertheless valid for our map, let us consider the map $g : I \to I$ defined as follows:

$$g : x \mapsto \; g(x) = \begin{cases} f_L(x) = x^{\alpha} & \text{for } 0 < x \le x_a, \\ f_C(x) = x_c^{\alpha} & \text{for } x_a < x \le x_c, \\ f_M(x) = \left[\frac{1}{\mu\beta}\left(1 - \frac{x}{m}\right)\right]^{\alpha/(1-\alpha)} & \text{for } x_c < x \le x_r, \\ f_R(x) = \widehat{x} & \text{for } x > x_r, \end{cases} \tag{27}$$

where $x_a = f_L^{-1}(x_r)$, $x_c = f_M^{-1}(x_r)$, $\widehat{x} = \left(\frac{1}{\beta}\right)^{\alpha/(1-\alpha)}$, $x_r = m(1-\mu)$, and parameters α, β, μ and m satisfy (2) and (20) (see an example of the map g in Fig.17). The map g is constructed from the map f by introducing a new flat branch $f_C(x)$ defined on the interval bounded by two preimages of the border point x_r, so that the absorbing interval of g is $J = [\widehat{x}, x_r]$ and the flat branch $f_R(x)$ plays no role for the dynamics. Clearly, the map g belongs to the class of maps considered in [28], thus, the U-sequence is valid for such a map (of course, to discuss the U-sequence in the map g we need to specify the related parameter path). On the other hand, it is easy to see that the map g is topologically conjugate to the considered map f, thus, the U-sequence is valid for it as well.

Before we describe the U-sequence of the map f let us recall in short how the standard U-sequence is formed using the logistic map $g : x \mapsto g(x) = ax(1-x)$, $3 < a < 4$, as an example. In [28] the U-sequence is constructed for the superstable cycles, for which the first letter in the symbolic sequence is C (corresponding to the point of maximum, separating the two partitions, L and R), and it is omitted. For example, the symbolic sequence of the superstable 3-cycle is $RL \equiv CRL$. Note that due to the fold bifurcation two 3-cycles are born, stable and unstable, with the same symbolic sequence, namely, RRL. Then, increasing a, at a suitable value the stable cycle becomes superstable, that is, it has the symbolic sequence CRL, and after we have the stable cycle with LRL sequence (which soon after becomes unstable via the flip bifurcation) while the unstable cycle, born in pair with the stable one, always persists with the sequence RRL. We can say that the sequence RL of the superstable 3-cycle *represents both the* 3-*cycles,* with the sequences LRL and RRL. As a different example consider the

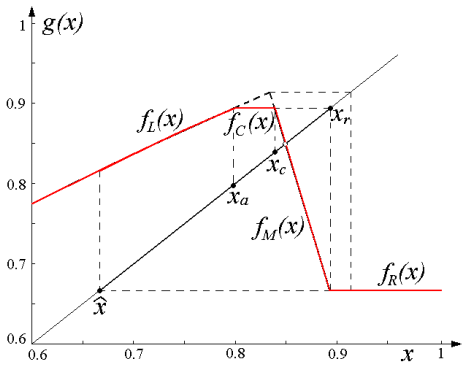

Figure 17: The map g defined in (27) at $m = 1.05$, $B = 1.5$, $\alpha = 0.5$ and $\mu = 0.15$.

sequence $RLR \equiv CRLR$ of the superstable 4-cycle. It *represents only one cycle*, namely, the 4-cycle with the symbolic sequence $RRLR$. Indeed, the sequence RLR is the first harmonic of R, that is, it represents the cycle born due to the period-doubling bifurcation of the 2-cycle.

The symbolic sequence of a superstable cycle of the logistic map which represents the one born at the fold bifurcation is called *fundamental*, while the symbolic sequences of the superstable cycles representing the cycles appearing due to the cascade of k period-doubling bifurcations, are called *k-harmonics*, $k > 0$. From [28] we recall that the (first) harmonic of a symbolic sequence σ is the sequence $\sigma\kappa\sigma$, where $\kappa = L$ if the number of R in σ is odd while $\kappa = R$ if this number is even. The k-harmonic is constructed by k consecutive applications of the same rule.

If we consider all the symbolic sequences of the logistic map related to its superstable cycles up to some period m, then these symbolic sequences belong to the U-sequence (the complete U-sequence includes all the admissible symbolic sequences of the superstable cycles of a unimodal map), and they are ordered for increasing values of the parameter a according to the following rule. For two different symbols $\kappa \neq \nu$, the order of κ and ν is in the sense of the natural order: $L < C < R$. Given two symbolic sequences $\sigma_1 = \sigma\kappa$ and $\sigma_2 = \sigma\nu$ with common string σ and next symbol $\kappa \neq \nu$, the order of σ_1 and σ_2 is the same (opposite) as the order of κ and ν if the number of R in σ is even (odd). For example, comparing two symbolic sequences of the superstable 4-cycles, $\sigma_1 = RL^2$ and $\sigma_2 = RLR$, we see that the number of R in their common string $\sigma = RL$ is odd, while the next symbols are L in σ_1 and R in σ_2, and $L < R$. Thus, we have that $RL^2 > RLR$.

The rule described above implies, in particular, that the symbolic sequence of the so-called basic n-cycle is the largest among the symbolic sequences of the

other n-cycles.[6] Recall that a basic n-cycle has only one symbol R in its symbolic sequence, that is, this sequence is RL^{n-2}. It can also be shown (see [28]) that the k- and $(k+1)$-harmonics of some symbolic sequence for any integer $k > 0$ are adjacent in the U-sequence (i.e., there are no any other symbolic sequences in between them). For example, the order of the symbolic sequences of the cycles of period $2 \leq n \leq 6$ of a unimodal map is the following :

$$\begin{aligned} R &< RLR < RLR^3 < RLR^2 < RL < RL^2RL < RL^2R < \\ RL^2R^2 &< RL^2 < RL^3R < RL^3 < RL^4, \end{aligned} \tag{28}$$

where the first or, equivalently, the last symbol, is C (which is omitted). Note that other symbolic sequences of higher periods exist between any two consecutive sequences but not between a sequence and its harmonic.

Let us now turn to the U-sequence observed in the map f. As we have already mentioned, we need first to specify an appropriate parameter path, which, roughly speaking, has to cross all the existing periodicity regions. Consider first the region E-I. As an appropriate parameter path in the (μ, β)-parameter plane (for values of α and m fixed as, for example, in the case shown in Fig.5) we can consider a cross-section of E-I from the right boundary FB_M to the left boundary $BC_{L,1}$. In the (μ, α)-parameter plane (for the values of B and m fixed as, for example, in the case shown in Fig.6) an appropriate parameter path can be the one connecting a point of the boundary FB_M with the organizing center O. Given that the map f for parameter values belonging to the region E-I is unimodal (and its cycles have symbolic sequences consisting of symbols L and M only), the order (28) is valid for f as well: we simply have to substitute the symbol R by M, while the first (omitted) symbol C corresponds to the symbol C_l :

$$\begin{aligned} M &< MLM < MLM^3 < MLM^2 < ML < ML^2ML < \\ ML^2M &< ML^2M^2 < ML^2 < ML^3M < ML^3 < ML^4. \end{aligned} \tag{29}$$

Note, however, that differently from the logistic map, the sequence given above is not related to the superstable cycles, but to the cycles one point of which is x_l. Some of these cycles can be stable (if the parameter path crosses the related periodicity region) and the other unstable.

Now we adjust the standard U-sequence to describe the cycles which can be observed in the map f when the parameters belong to the region E-II. An appropriate parameter path has to cross all the periodicity regions of superstable cycles. For example, we can vary the parameter values along an arc connecting the point marked by s_1 in Fig.6a with the organizing center O. In each of the symbolic sequences constituting the order (29), the first symbol M corresponding to the maximal periodic point, has to be substituted by R (and, as we have

[6] For a prime period $n > 2$ the number of stable n-cycles having different symbolic sequences is $k(n) = (2^{n-1} - 1)/n$. For the generic case see, e.g., [17].

already noticed, only one point R can exist in a symbolic sequence):

$$\begin{aligned} R &< RLM < RLM^3 < RLM^2 < RL < RL^2ML < \\ RL^2M &< RL^2M^2 < RL^2 < RL^3M < RL^3 < RL^4. \end{aligned} \tag{30}$$

Such a sequence corresponds to the order of the superstable cycles of f one point of which is x_l, with the symbol C_l omitted in the above order. The generic rule recalled above to determine the order of such sequences, has to be modified taking into account that one letter R takes the place of one letter M in the standard U-sequence. So, the rule for the order (30) is as follows. Given two different symbols $\kappa \neq \nu$, the order of κ and ν is, as before, in the sense of the natural order: $L < C_l < M$. Given two symbolic sequences $\sigma_1 = \sigma\kappa$ and $\sigma_2 = \sigma\nu$ with common string σ and next symbol $\kappa \neq \nu$, the order of σ_1 and σ_2 is the same (opposite) as the order of κ and ν if the number of M in σ is odd (even).

Let us now extend the order (30) to all the superstable cycles of the map f (i.e., not only those with periodic point x_l). As we have seen, the curves corresponding to the cycles with point x_l are related to the persistence border collisions and located inside the periodicity regions of the corresponding superstable cycles. In some sense, these curves constitute a skeleton of the overall "superstable" bifurcation structure, quite similar to the parameter values of the superstable cycles of the logistic map, located inside the related periodicity windows. To construct the complete sequence we can substitute each symbolic sequence σ by two new sequences, σL and σM, ordered according to the rule stated above. For example, the sequence R related to the superstable 2-cycle RC_l can be substituted by two sequences, RM and RL (representing the related superstable 2-cycles) ordered as $RM < RL$. The sequence RLM representing superstable 4-cycle $RLMC_l$ can be substituted by $RLML$ and $RLMM$ ordered as $RLML < RLMM$ (cf. with (23)). One more example is the sequence $RL \equiv RLC_l$ representing the superstable 3-cycle which can be substituted by $RLM < RLL$.

Thus, the complete order of the superstable cycles periods $2 \leq n \leq 6$ of the map f is the following:

$$\begin{aligned} &RM < RL < RLML < RLM^2 < RLM^3L < RLM^4 < \\ &RLM^3 < RLM^2L < RLM < RL^2 < RL^2ML^2 < RL^2MLM < \\ &RL^2ML < RL^2M^2 < RL^2M^3 < RL^2M^2L < RL^2M < RL^3 < \\ &RL^3ML < RL^3M^2 < RL^3M < RL^4 < RL^4M < RL^5. \end{aligned} \tag{31}$$

To summarize, we have obtained an analogue of the U-sequence according to which the periodicity regions related to the superstable cycles of the map f defined in (9) are ordered. These periodicity regions belong to the parameter region $E\text{-}II$ given in (20) related to the map f defined over the absorbing interval via three functions one of which is a constant. The bifurcation structure in the parameter region $E\text{-}I$ given in (19) as well as the periodicity regions belonging to $E\text{-}II$ but not related to the superstable cycles, is discussed in a forthcoming paper.

ACKNOWLEDGMENTS

This work has been performed within the activity of the project PRIN 2009 "Local interactions and global dynamics in economics and finance: models and tools", MIUR, Italy, and under the auspices of COST Action IS1104 "The EU in the new complex geography of economic systems: models, tools and policy evaluation".

References

[1] V. Avrutin, M. Schanz, Multi-parametric bifurcations in a scalar piecewise-linear map, Nonlinearity 19 (2006) 531–552.

[2] V. Avrutin, B. Futter, and M. Schanz. The discontinuous top tent map and the nested period incrementing bifurcation structure. Chaos, Solitons & Fractals, 45 (2012) 465–482.

[3] V. Avrutin, B. Futter, L. Gardini and M. Schanz. Unstable orbits and Milnor attractors in the discontinuous flat top tent map, ESAIM (European Series in Applied and Industrial Mathematics), 36 (2012) 126-158.

[4] V. Avrutin, I. Sushko. A gallery of bifurcation scenarios in piecewise smooth 1D maps. In: *Global analysis of dynamic models for economics, finance and social sciences* (G.-I. Bischi, C. Chiarella and I. Sushko Ed.s), Springer, 2013.

[5] S. Banerjee, G.C. Verghese (eds), Nonlinear Phenomena in Power Electronics: Attractors, Bifurcations, Chaos, and Nonlinear Control, IEEE Press, New York, 2001.

[6] Bischi, G. I., Chiarella, C., Kopel, M., and Szidarovszky, F. (2009). Nonlinear oligopolies: Stability and bifurcations. Heidelberg: Springer.

[7] G.I. Bischi, L. Gardini, U. Merlone, Impulsivity in binary choices and the emergence of periodicity, Discrete Dynamics in Nature and Society, Article ID 407913, 22 pages, doi:10.1155/2009/407913 (2009).

[8] S. Brianzoni, E. Michetti, I. Sushko. Border Collision Bifurcations of Superstable Cycles in a One-Dimensional Piecewise Smooth Map. *Mathematics and Computers in Simulation,* Vol. 81, Issue 1 (2010), 52-61.

[9] B. Brogliato. Nonsmooth Mechanics – Models, Dynamics and Control. Springer–Verlag, New York, 1999.

[10] A. Dal Forno, L. Gardini, U. Merlone, Ternary choices in repeated games and border collision bifurcations, Chaos Solitons & Fractals, 45 (2012) 294–305

[11] R. Day, Complex Economic Dynamics, MIT Press, Cambridge, 1994.

[12] W. de Melo and S. van Strien, One-Dimensional Dynamics, Springer Verlag, New York, 1991.

[13] M. di Bernardo, C.J. Budd, A.R. Champneys, P. Kowalczyk, Piecewise-smooth Dynamical Systems: Theory and Applications. Applied Mathematical Sciences 163. Springer-Verlag, London, 2007.

[14] Gardini L., I.Sushko and A. Naimzada, Growing Through Chaotic Intervals, Journal of Economic Theory, 143 (2008) 541-557.

[15] L. Gardini, I. Sushko, V. Avrutin, M. Schanz. Critical homoclinic orbits lead to snap-back repellers. Chaos, Solitons & Fractals, 44 (2011) 433–449.

[16] L. Gardini, U. Merlone, F. Tramontana, Inertia in binary choices: continuity breaking and big-bang bifurcation points, Journal of Economic Behavior & Organization 80 (2011) 153– 167.

[17] B.L. Hao, Elementary Symbolic Dynamics and Chaos in Dissipative Systems, World Scientific, Singapore, 1989.

[18] Hommes, C., Nusse H., "Period three to period two" bifurcation for piecewise linear models, J. Economics, 54, 2 (1991), 157-169.

[19] Huang, W. and Day, R. (1993), Chaotically switching bear and bull markets: the derivation of stock price distributions from behavioral rules. In: Day, R. and Chen, P. (Eds.): Nonlinear Dynamics and Evolutionary Economics, Oxford University Press, Oxford, 169-182.

[20] S. Ito, S. Tanaka, H. Nakada, On unimodal transformations and chaos II, Tokyo J. Math. 2 (1979) 241-259.

[21] N.N. Leonov, Map of the line onto itself, Radiofisica 3 (1959) 942–956.

[22] Y.L. Maistrenko, V.L. Maistrenko, L.O. Chua, Cycles of chaotic intervals in a time-delayed Chua's circuit, Int. J. Bifurcat. Chaos 3 (1993) 1557–1572.

[23] K. Matsuyama (2001), Good and Bad Investment: An Inquiry into the Causes of Credit Cycles, Center for Mathematical Studies in Economics and Management Science Discussion Paper No.1335, Northwestern University.

[24] K. Matsuyama (2004), The Good, The Bad, and The Ugly: An Inquiry into the Causes and Nature of Credit Cycles, Center for Mathematical Studies in Economics and Management. Science Discussion Paper No.1391, Northwestern University.

[25] K. Matsuyama, Credit Traps and Credit Cycles, American Economic Review, 97 (2007) 503-516.

[26] K. Matsuyama (2012), The Good, The Bad, and The Ugly: An Inquiry into the Causes and Nature of Credit Cycles. Theoretical Economics (forthcoming).

[27] K. Matsuyama (2012), Chaotic Credit Cycles. Presentation at "Money, Banking, Payments and Finance Workshop" Federal Reserve Bank of Chicago, August 2012 (Downloadable from http://faculty.wcas.northwestern.edu/~kmatsu/).

[28] N. Metropolis, M.L. Stein and P.R. Stein, On finite limit sets for transformations on the unit interval, J. Comb. Theory 15 (1973), 25-44.

[29] J. Milnor. On the Concept of Attractor. Commun. Math. Phys. 99, 177-195 (1985) 177-195.

[30] H.E. Nusse, J.A. Yorke, Border-collision bifurcations including period two to period three for piecewise smooth systems, Physica D 57 (1992) 39-57.

[31] H.E. Nusse, J.A. Yorke, Border-collision bifurcation for piecewise smooth one-dimensional maps, Int. J. Bifurcation Chaos 5 (1995) 189-207.

[32] T. Puu, I. Sushko, Oligopoly Dynamics, Models and Tools, Springer Verlag, New York, 2002.

[33] T. Puu, I. Sushko, Business Cycle Dynamics, Models and Tools, Springer Verlag, New York, 2006.

[34] I. Sushko, A. Agliari, L. Gardini. Bifurcation Structure of Parameter Plane for a Family of Unimodal Piecewise Smooth Maps: Border-Collision Bifurcation Curves. Dynamic Modelling in Economics and Finance in honour of Professor Carl Chiarella (G.I. Bischi and I. Sushko Ed.s), Chaos, Solitons & Fractals, Vol. 29, Issue 3 (2006), 756-770.

[35] I. Sushko, L. Gardini, Degenerate Bifurcations and Border Collisions in Piecewise Smooth 1D and 2D Maps, Int. J. Bif. and Chaos 20 (2010) 2045-2070.

[36] F. Tramontana, L. Gardini, T. Puu, Mathematical Properties of a combined Cournot-Stackelberg model, Chaos, Solitons & Fractals, 44 (2011) 58-70.

[37] F.Tramontana, F.Westerhoff, L.Gardini, On the complicated price dynamics of a simple one-dimensional discontinuous financial market model with heterogeneous interacting traders, J. Econ. Behav. Organ. 74 (2010) 187–205.

[38] F.Tramontana, L.Gardini, F.Westerhoff, Heterogeneous speculators and asset price dynamics: further results from a one-dimensional discontinuous piecewise-linear model, Computational Economics, 38 (2011) 329–347.

[39] Z.T. Zhusubaliyev, E. Mosekilde, Bifurcations and Chaos in Piecewise-Smooth Dynamical Systems, World Scientific, Singapur, 2003.